emical Physics 41 (1979) 163–181
North-Holland Publishing Company

PHENOMENOLOGY OF RESONANCE RAMAN SCATTERING AND RESONANCE FLUORESCENCE FROM THERMALLY RELAXING SYSTEMS*

Abraham NITZAN
Department of Chemistry, Tel-Aviv University, Tel Aviv, Israel

Received 8 December 1978

The problem of resonance Raman scattering and resonance fluorescence from thermally relaxing systems is studied. A general expression obtained earlier is rewritten explicitly in the dipole approximation. Numerical computations are performed on simple model systems and reveal the role that thermal relaxation play in the light scattering process. In particular, the effect of thermal relaxation on interference features, the temperature dependence of the absorption and the scattering cross-sections (apart from the effect of the initial level distribution) and the transition from thermal relaxation behavior to an irreversible damping are studied in detail.

1. Introduction

In the past few years we have witnessed a revival of the interest in the foundations of resonance Raman scattering†, induced by the advances in experimental techniques which make it possible to tune the exciting laser light in the vicinity of resonances. Three main subjects have been the focus of recent experimental and theoretical studies in the foundations of the Raman scattering process. (a) Effects of thermal relaxation processes and the distinction between resonance Raman scattering (RRS) and resonance fluorescence (RF) [2–15]. (b) The relation of the absorption lineshape to the Raman scattering spectrum and the effects of interference between different intermediate levels on variations in the relative absorption/scattering intensity [16–26]. (c) The effects of strong incident radiation fields and non-linear phenomena [27] (see also ref. [3] and references therein).

From the operational point of view, the light scattering process may be followed either in the time domain (time resolved or short time experiments) or in the energy domain (energy resolved long time experiments). Both classes contain in principle the same amount of information. In the present paper I limit myself to the weak field energy resolved situation whereupon the idealized experimental configuration involves a low intensity beam of polarized monochromatic light incident on the system under study. The adsorption and the scattering spectra are monitored under high resolution together with the polarization of the scattered light. Information is usually obtained from the following observables: (a) Absorption lineshapes, (b) scattering lineshapes, (c) energy resolved quantum yields (ratio between adsorption and scattering intensities) and finally (d) energy resolved depolarization ratios, reversal factors and circularity parameters.

When an incident low intensity light interacts with a system (henceforth referred to as a molecule) which in turn interacts with its thermal environment, the scattered light contains in general three different components (fig. 1): (a) coherent Raman components, (b) direct (resonance) fluorescence lines resulting from the excited level

* Supported in part by the Commission for Basic Research of the Israel Academy of Sciences.
† For reviews, see ref. [1]. For a list of recent references see refs. [2–4].

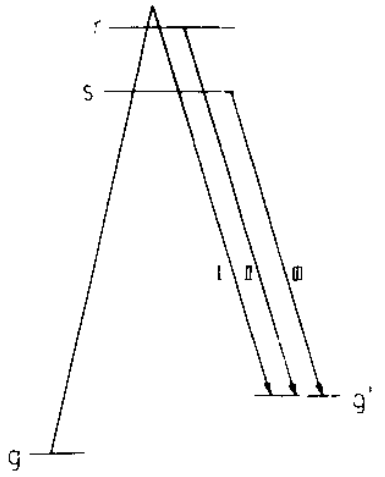

Fig. 1. A schematic representation of the three components of scattered light from a thermally relaxing system. The Raman lines (I) correspond to exact energy conservation between the molecule and the radiation field. The direct fluorescence lines (II) result mainly from phase relaxation while transfer lines (III) originate from population relaxation.

approximately in resonance with the incident beam, (c) transfer fluorescence lines – emission from levels which are populated by the thermal relaxation. Both direct and transfer fluorescence result from the thermal interaction between the system and its surroundings and vanish when this interaction disappears, leaving the usual Raman scattering off an isolated molecule. In the other extreme case of very fast relaxation within a given group of excited molecular levels, the emission will be completely relaxed. Analysis of the observables listed above may yield valuable information on intramolecular and intermolecular relaxation processes.

In the present paper I follow the convention which uses the terms Raman (coherent) scattering and fluorescence (incoherent scattering) for the response of the molecule to the incident radiation field prior to and following thermal relaxation respectively[†]. In a long time experiment these components are distinguishable only by the corresponding scattered photon energy (fig. 1). In some works (see e.g., ref. [29]) the terms RF and RRS refer respectively to cases where a single or many intermediate levels contribute to the scattering intensity. It seems that the former distinction serves a better purpose as the coherent and the incoherent scattering components are qualitatively different.

Several years ago we had analyzed interference effects in resonance Raman scattering from isolated (low pressure gas phase) large molecules [16]. It had been concluded that whereas in the isolated resonance case the absorption and the scattering cross section are exactly proportional to each other (so that the energy resolved quantum yield function is constant), interference between several resonances, or between a discrete level and a continuum lead to a marked deviation from this behavior. This conclusion has since then been reached by other workers and was verified experimentally [20–26]. In this connection it is worthwhile to mention that interference phenomena in RRS may result from two factors: The conventional expression for the total Raman scattering cross section is (with antiresonant terms disregarded)

$$(\sigma_{\lambda\nu})_{g\to g'} \propto \frac{\omega'}{\omega_0}\left|\sum_a \omega_{ag}\omega_{ag'}\frac{(\mu_\lambda)_{g'a}(\mu_\nu)_{ag}}{E_g + E_0 - E_a + i\gamma_a}\right|^2, \qquad (1)$$

where $|g\rangle$ is the initial molecular level, $|g'\rangle$ – the final one and where $\{|a\rangle\}$ are intermediate levels; μ is the electronic dipole moment operator (μ_ν denotes the ν spatial component); $E_0 = \hbar\omega_0$ is the energy of the incident photon and $E' = \hbar\omega'$ is the energy of the scattered one; E_j ($j = g, g', a$) is the energy of the molecular level j. Finally γ_j is the half-width of the molecular level j; the damping matrix γ is assumed to be diagonal in the set of molecular wavefunctions. Eq. (1) obviously leads to cross-coupling terms between different resonances. It should be noticed that the corresponding absorption cross section is given by a simple sum of lorentzian functions

[†] In refs. [7–10] the term luminescence is used rather than fluorescence.

$$\sigma_g \propto \frac{1}{\omega_0} \sum_a \omega_{ag}^2 |\mu_{ag}|^2 \frac{\gamma_a}{(E_g + E_0 - E_a)^2 + \gamma_a^2}, \tag{2}$$

with no inherent interference effects. Interference phenomena in RRS are usually analysed using eq. (1).

Another source for interference in RRS is the possible nondiagonality of the damping matrix γ. In fact, whenever resonances are close enough so that they do not contribute separately in eq. (1), this possibility should be considered. When γ is non-diagonal eqs. (1) and (2) are no longer valid and interference effects appear also in the absorption lineshape function. A proper treatment of interference effects in RRS should start from a more general expression for the polarizability [16] or provide a justification for utilizing a diagonal damping matrix. (A diagonal damping matrix results if the interfering states are damped by coupling to independent damping channels, also when the coupling of these states to the damping channel is random as is the case for radiationless electronic transitions in large molecules [29, 30].)

Turning to the problem of resonance light scattering from multilevel, thermally relaxing systems, the following questions are pertinent.

(1) How do different relaxation processes affect the observables associated with the scattering experiment? The relaxation processes involved are (a) intramolecular damping (radiationless electronic transitions) which is an important decay route in large molecules; (b) environmentally (e.g. collisions) induces radiationless electronic transitions; (c) radiative decay; (d) environmentally induced vibrational and rotational relaxation; and finally (e) environmentally induced dephasing processes.

(2) How are the coherent (Raman) and the incoherent (fluorescence) part of the scattered light affected by the different intramolecular and intermolecular (thermal) relaxation processes?

(3) How does the thermal interaction of the system with its surroundings affect the observations of interference effects of the kind discussed above?

(4) How are the relevant observables affected by the temperature of the surrounding medium?

(5) To what extent can quantitative information about the molecule–medium interaction and the molecular relaxation rates be extracted from the resonance light scattering experiment?

Turning to a closer examination of the relaxation processes listed above, we notice that these can be separated into two classes – reversible and irreversible. The spontaneous radiative decay of molecular levels is, in most relevant cases, irreversible[†]. So is the intramolecular radiationless electronic transitions in large molecules belonging to the so called statistical limit. Vibrational and rotational relaxation are reversible processes at room temperature. Collision induced electronic transitions may be reversible or irreversible depending on the electronic energy gap associated with the transition. Both reversible and irreversible relaxation processes may be treated in a unified way as thermal relaxation processes: Each process is associated with an interaction of the molecule with a certain thermal bath which for irreversible processes is taken as a zero temperature bath. Thus, apart from the incident mode, the radiation field is assumed to be in its vacuum (zero temperature) state which leads to irreversible radiative decay. Vibrational and rotational relaxation are governed by the temperature of the translational bath. Intramolecular and usually also collision induced radiationless electronic relaxation processes are associated with large energy gaps and effectively zero temperature baths[††].

As we shall see, the coupling of intermediate levels to zero temperature or to finite temperature baths affect light scattering processes in qualitatively different ways. In particular a zero temperature bath cannot induce

[†] By "relevant" I mean cases where the spontaneous radiative decay occurs on an experimentally relevant time scale. By "irreversible" I mean unidirectional damping as opposed to thermal relaxation at finite temperature.

[††] For intramolecular relaxation the molecular vibrational levels of a lower electronic manifold constitute this bath. It should be noticed that in most cases the bath is the thermal environment of the system. If however relaxation processes between levels with large energy separations ($\Delta E \gg k_B T$) do not correlate with those between more closely seated levels, we can regard the former as induced by an independent zero temperature bath.

proper dephasing (T_2 type) processes but only population changes (T_1 type relaxation) while a finite temperature bath can induce both.

Mukamel and Nitzan [4] have considered the general problem of RRS and RS from multilevel systems which interact thermally with its surroundings. Their approach and main results are summarized and extended in section 2. Section 3 presents the results of a numerical study on model systems which provide simple examples for the interplay between interference effects and thermal effects in resonance light scattering processes. The theoretical results and the numerical study lead to the following conclusions:

(1) Interference effects are manifested most strongly in the incident energy dependence of the quantum yield Y and of the ratio R between the integrated RRS and fluorescence (F) cross sections.

(2) Thermal relaxation smears out interference features. The effect is more pronounced in the quantum yield and in the RRS F ratio spectra.

(3) The effect of the two thermal processes: Level dephasing and population cross-relaxation, on features observed as functions of incident energy are very similar in the high temperature limit. The effects on features observed as functions of scattered energy are quite different. In particular, the first enhances direct fluorescence lines while the second enhances transfer lines.

(4) The fluorescence cross section, displayed either as a function of incident or as a function of scattered energy, shows no interference character even when the absorption lineshape and the RRS component show a marked interference behavior.

(5) Broadening due to irreversible damping is qualitatively different from thermal broadening: Increasing the damping relative to energy spacing in the intermediate manifold leads to interference behavior while increasing the thermal broadening does not.

(6) As irreversible damping processes become more efficient, the ratio R between the integrated RRS and F cross sections increases.

(7) As the temperature becomes comparable to or lower than the energy spacing in the intermediate manifold the absorption and excitation spectra may become asymmetric. The ratio R increases and becomes relatively larger on the low energy side of the spectrum.

By fitting experimental results to the theoretical expressions for the absorption and scattering cross sections, for their ratios and for relative intensity of direct and transfer lines, quantitative information may be obtained for the molecular relaxation rates.

2. The thermally averaged observables of the scattering process

In this section I summarize and extend the main results obtained by Mukamel and Nitzan [4] on RRS from thermally relaxing systems. The model employed is characterized by the following features:

(a) The molecular system is represented by a set of relevant energy levels (fig. 2). This set may be divided

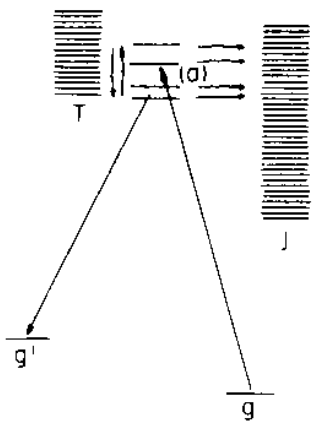

Fig. 2. Energy level model for light scattering off a thermally relaxing system. The continuum T denotes a thermal bath of temperature T. The continuum seated on the level j is one of several zero temperature baths which represents channels for irreversible damping. $\{a\}$ is the manifold of optically active levels interacting with the baths. g and g' are the initial and final states of the scattering process.

into three groups. First, the initial $|g\rangle$ and the final $|g'\rangle$ levels belonging to the ground electronic manifold. Secondly a manifold A which contains those levels $\{|a\rangle\}$ which are in resonance with the incident light together with levels which may be populated and fluoresce in the course of the thermal relaxation process. In common situations the manifold A contains the optically active levels of an intermediate electronic state which is in resonance with the incident light. Finally these levels may interact with a manifold J of levels belonging to lower electronic states. In the statistical limit this leads to an irreversible decay of the $|a\rangle$ levels.

(b) The levels $|a\rangle$ are coupled to each other by the interaction between the molecule and a thermal bath of temperature T. Obviously, all levels which are efficiently coupled by this interaction and whose energy separation from the resonance region does not greatly exceed $k_B T$ should be included in manifold A. However, levels which loose their population very rapidly due to further relaxation processes should be taken as part of the manifold J. Such is the case when collisions induce irreversible transitions between electronic manifolds in small and intermediate size molecules.

It should be noticed that the manifold J may be regarded as a special case of a thermal bath of zero temperature seated on some optically inactive molecular level which lies far below the resonance region. With this viewpoint, thermal interaction and irreversible damping may be treated on the same footing.

(c) The separation approximation [11] is adopted in the calculation of the thermally averaged scattering process. In most model calculations presented in the present article I invoke also the impact approximation [12] for the system–thermal bath interaction.

(d) The thermal interaction may cause both population changes (T_1 processes) and level dephasing (proper T_2 processes). It is assumed that these different processes are uncorrelated.

(e) The scattering process is described in terms of the levels $|g\rangle$ and $|g'\rangle$ of the ground electronic manifold. The actual observed spectrum is of course a superposition of spectra which belong to different final $|g'\rangle$ levels, each averaged over a thermal distribution of initial levels $|g\rangle$. In many cases it is indeed possible to separate contributions belonging to different given $|g\rangle - |g'\rangle$ pairs.

(f) The incident intensity is assumed to be low enough, so that the lowest order perturbation term (in the molecule interaction with the incident mode) necessary for the calculation of any observable, is sufficient. Radiative decay of the molecular $|a\rangle$ levels may be taken into account – the radiation field (apart from the incident mode) provides a zero temperature bath for this process.

The model described above leads to the following results [4]:

(a) The absorption cross section for a linearly polarized incident monochromatic light in vacuum is given by

$$\sigma_g = (i\Omega/c\hbar)\boldsymbol{a}^+ \mathbf{M} \boldsymbol{a}, \tag{3}$$

where $\boldsymbol{a}$ is a $2n$ dimensional vector (n being the number of levels in the manifold A) whose elements are

$$\boldsymbol{a}^+ = (V^*_{ga_1} \ldots V^*_{ga_n}, -V^*_{a_1 g} \ldots -V^*_{a_n g}), \tag{4}$$

where in the dipole approximation†

$$V_{lj} = -i\omega_{lj}(4\pi\hbar/\Omega\omega_0)^{1/2}\, \boldsymbol{\mu}_{lj} \cdot \boldsymbol{e} = V^*_{jl}, \tag{4a}$$

$$\omega_{lj} = \hbar^{-1}(E_l - E_j); \quad l, j\text{-molecular levels.} \tag{4b}$$

$\boldsymbol{\mu}_{lj}$ is the matrix element of the molecular dipole moment operator and $\boldsymbol{e}$ is the polarization vector (unit vector in the direction of the electric field) of the incident radiation. ω_0 is the frequency of the incident light, Ω is the normalization volume for the radiation and c is the speed of light in vacuum. The matrix $\mathbf{M}$ is given by

† The constants appearing in eq. (4a) correspond to the CGS system of units. Note that in the equations of section 4 of ref. [4] the complex conjugate notation is erroneously missing in some equations.

$$\mathbf{M} = \begin{pmatrix} E_{a_1 g} - E_0 + \bar{R}_{a_1 g, a_1 g} & \bar{R}_{a_1 g, a_2 g} & \cdots & R_{a_1 g, a_n g} & \bar{R}_{a_1 g, g a_1} & \cdots & \bar{R}_{a_1 g, g a_n} \\ \bar{R}_{a_2 g, a_1 g} & E_{a_2 g} - E_0 + \bar{R}_{a_2 g, a_2 g} & & & & & \vdots \\ \vdots & & \ddots & & & & \\ \bar{R}_{a_n g, a_1 g} & & & & & & \\ \bar{R}_{g a_1, a_1 g} & & & & & & \\ \vdots & & & & & & \\ \bar{R}_{g a_n, a_1 g} & \cdots & & \cdots & \cdots & & E_{g a_n} + E_0 + \bar{R}_{g a_n, g a_n} \end{pmatrix} \tag{5}$$

The numbers $\bar{R}$ are defined in terms of the operators

$$U_{\mathrm{B}} = \sum_{ll'} U_{\mathrm{B}}^{ll'} |l\rangle\langle l'|. \tag{6}$$

U_{B} is the interaction between the molecule characterized by levels $\{|l\rangle\}$ and the thermal bath B. $U_{\mathrm{B}}^{ll'} = \langle l| U_{\mathrm{B}} |l'\rangle$ in eq. (7) are operators in the bath coordinates. The numbers $\bar{R}$ are given in the Born approximation in terms of equilibrium correlation functions of these operators

$$\bar{R}_{ab,cd} = -\mathrm{i} \int_{-\infty}^{\infty} \mathrm{d}t \sum_{\mathrm{B}} \Big\{ \delta_{bd} \sum_l \exp(-\mathrm{i}E_{lb}t) \langle U_{\mathrm{B}}^{al}(t)\, U_{\mathrm{B}}^{lc}(0)\rangle + \delta_{ac} \sum_l \exp(-\mathrm{i}E_{al}t) \langle U_{\mathrm{B}}^{dl}(0)\, U_{\mathrm{B}}^{lb}(t)\rangle$$

$$- \exp(-\mathrm{i}E_{cb}t) \langle U_{\mathrm{B}}^{db}(0)\, U_{\mathrm{B}}^{ac}(t)\rangle - \exp(-\mathrm{i}E_{ad}t) \langle U_{\mathrm{B}}^{db}(t)\, U_{\mathrm{B}}^{ac}(0)\rangle \Big\}. \tag{7}$$

The different terms contributing to $\bar{R}$ constitute the set of thermal rates which govern the thermal relaxation process (population relaxation and dephasing) undergone by the molecule. Explicit expressions for these rates for a two intermediate levels system are summarized below.

Eq. (3) should be averaged over all molecular orientations with the directional information implied by eq. (4a). Obviously, if the transition dipoles $\boldsymbol{\mu}_{ga_i}$ and $\boldsymbol{\mu}_{ga_j}$ are perpendicular to each other, the absorption cross section cannot contain interference contributions from these two levels. Here, I am interested in discussing thermal relaxation effects on interference phenomena and I therefore consider the extreme case in which the transition dipoles $\boldsymbol{\mu}_{ga}$ for all a are parallel to each other. Also, as $\omega_0 \approx \omega_{ga} \gg \omega_{a'a''}$ for all a, a', a'', I can replace ω_{ga} by ω_0 in eq. (4a). I consider a non-polarized incident beam and average σ_g over all incident polarizations. This leads to

$$\sigma_g = -2\pi\mathrm{i}\omega_0 c^{-1} \bar{\boldsymbol{a}}^{+} \mathbf{M} \bar{\boldsymbol{a}}, \tag{8}$$

with

$$\bar{\boldsymbol{a}}^{+} = (\mu_{ga_1} \cdots \mu_{ga_n}, \mu_{a_1 g} \cdots \mu_{a_n g}). \tag{9}$$

(b) The scattering cross section under the same condition $\omega_0, \omega' \gg \omega_{a'a''}$ described above, where the incident field is linearly polarized in the δ direction and the scattered field is observed with λ polarization is given by

$$(\sigma_{\lambda\nu})_{g \to g'} = -\mathrm{i} \frac{16\pi^2 \hbar}{c\Omega} \omega_0 \omega' \times \bar{\boldsymbol{b}}_{\lambda}^{+} \mathbf{N} [(\mathbf{A}_1)_{\lambda} \mathbf{K}_1 (\bar{\mathbf{B}}_1)_{\nu} + (\bar{\mathbf{A}}_2)_{\nu} \mathbf{K}_2 (\bar{\mathbf{B}}_2)_{\lambda}] \mathbf{M} \boldsymbol{a}_{\nu}, \tag{10}$$

where $\mathbf{M}$ is given by eq. (5), $\mathbf{N}$ is identical to it only that g' replaces g and E' replaces E_0, everywhere. The matrix $\mathbf{K}_1$ is an $n^2 \times n^2$ square matrix given by

$$\mathbf{K}_1 = -\begin{pmatrix} \boldsymbol{\kappa}^{(11)} \cdots \boldsymbol{\kappa}^{(1n)} \\ \vdots \\ \boldsymbol{\kappa}^{(n1)} \cdots \boldsymbol{\kappa}^{(nn)} \end{pmatrix}, \tag{11}$$

where $\boldsymbol{\kappa}^{(ij)}$ is an $n \times n$ square matrix of the form

$$\kappa_{lm}^{(ij)} = (E_{a_i} - E_{a_j})\delta_{ij}\delta_{lm} + \bar{R}_{a_i a_l, a_j a_m}. \tag{12}$$

The matrix $\mathbf{K}_2$ is the 2×2 diagonal matrix

$$\mathbf{K}_2 = \begin{pmatrix} (E_{g'g} - \bar{R}_{gg',gg'})^{-1} & 0 \\ 0 & (E_{gg'} - \bar{R}_{g'g,g'g})^{-1} \end{pmatrix}. \tag{13}$$

The other vectors and matrices appearing in eq. (10) are

$$\bar{\boldsymbol{a}}_\nu = \begin{pmatrix} \mu_{a_1 g} \\ \vdots \\ \mu_{a_n g} \\ \mu_{g a_1} \\ \vdots \\ \mu_{g a_n} \end{pmatrix}_\nu \qquad (2n \text{ column vector}), \tag{14}$$

$$\bar{\boldsymbol{b}}_\lambda^+ = (\mu_{g'a_1} \cdots \mu_{g'a_n} \ \mu_{a_1 g'} \cdots \mu_{a_n g'})_\lambda \qquad (2n \text{ row vector}), \tag{15}$$

$$(\bar{\mathbf{B}}_2)_\lambda = \begin{pmatrix} 0 & \cdots & 0 & \mu_{a_1 g'} & \cdots & \mu_{a_n g'} \\ \mu_{g'a_1} & \cdots & \mu_{g'a_n} & 0 & \cdots & 0 \end{pmatrix}_\lambda \qquad (2 \times 2n \text{ matrix}), \tag{16}$$

$$(\bar{\mathbf{A}}_2)_\nu = \begin{pmatrix} \mu_{a_1 g} & 0 \\ \vdots & \vdots \\ \mu_{a_n g} & 0 \\ 0 & \mu_{g a_1} \\ \vdots & \vdots \\ 0 & \mu_{g a_n} \end{pmatrix}_\nu \qquad (2n \times 2 \text{ matrix}), \tag{17}$$

$$(\bar{\mathbf{B}}_1)_\nu = \begin{pmatrix} \boldsymbol{\beta}^{(11)} & \boldsymbol{\beta}^{(12)} \\ \vdots & \vdots \\ \boldsymbol{\beta}^{(n1)} & \boldsymbol{\beta}^{(n2)} \end{pmatrix}_\nu \qquad (n^2 \times 2n \text{ matrix}), \tag{18}$$

$\boldsymbol{\beta}^{(lm)}$ are $n \times n$ square matrices given by $\beta_{ij}^{(11)} = \delta_{jl}\mu_{g a_i}$, $\beta_{ij}^{(12)} = \delta_{ij}\mu_{a_l g}$, (19)

$$(\bar{\mathbf{A}}_1)_\lambda = \begin{pmatrix} \boldsymbol{\alpha}^{(11)} & \cdots & \boldsymbol{\alpha}^{(1n)} \\ \vdots & & \vdots \\ \boldsymbol{\alpha}^{(21)} & \cdots & \boldsymbol{\alpha}^{(2n)} \end{pmatrix} \qquad (2n \times n^2 \text{ matrix}). \tag{20}$$

$\boldsymbol{\alpha}^{(lm)}$ are $n \times n$ square matrices with elements

$$\alpha_{ij}^{(m)} = \delta_{im}\mu_{a_j g'}, \qquad \alpha^{(2m)} = \delta_{ij}\mu_{g' a_m}. \tag{21}$$

The subscripts λ and ν appearing in eqs. (14)–(20) denote that it is the corresponding λ (or ν) component of $\boldsymbol{\mu}$ which is to be taken in all terms of the vector or matrix. Multiplying eq. (10) by the number of modes available to the scattered beam in the range $\mathrm{d}\omega'$ of the final frequencies and in a solid angle $\mathrm{d}\tau$

$$N(\omega') = \rho(\omega')\,\mathrm{d}\omega'\,\mathrm{d}\tau = \Omega\omega'^2(2\pi c)^{-3}\,\mathrm{d}\omega'\,\mathrm{d}\tau \tag{22}$$

leads to the final general result for the differential scattering cross section

$$\frac{\mathrm{d}^2(\sigma_{\lambda\nu})_{g\to g'}}{\mathrm{d}\omega'\,\mathrm{d}\tau} = -\mathrm{i}\,\frac{2\hbar}{\pi c^4}\,\omega_0(\omega')^3 \times \bar{\boldsymbol{b}}_\lambda^+ \mathbf{N}[(\bar{\mathbf{A}}_1)_\lambda \mathbf{K}_1 (\mathbf{B}_1)_\nu + (\bar{\mathbf{A}}_2)_\nu \mathbf{K}_2 (\bar{\mathbf{B}}_2)_\lambda]\mathbf{M}\boldsymbol{a}_\nu. \tag{23}$$

If we make the additional assumptions that all the elements of the dipole moment operator are parallel to each other, that the incident field is unpolarized and that all polarization components of the scattered light are collected by the detector, we obtain a result of the form (23) with $(\mathbf{A}_1)_\lambda$, $(\mathbf{B}_1)_\nu$, $(\mathbf{A}_2)_\nu$ and $(\mathbf{B}_2)_\lambda$ replaced by $\bar{\mathbf{A}}_1$, $\bar{\mathbf{B}}_1$, $\bar{\mathbf{A}}_2$ and $\bar{\mathbf{B}}_2$, in which the absolute magnitude of μ replaces the ν and λ components and with additional factor of 1/2 (resulting from the average over the initial polarization). The final result for the scattering cross section under these conditions is

$$\left(\frac{\mathrm{d}^2\sigma_{g\to g'}}{\mathrm{d}\omega'\,\mathrm{d}\tau}\right)\mathrm{d}\omega'\,\mathrm{d}\tau = -\mathrm{i}\frac{\hbar}{\pi c^4}\omega_0\omega'^3\bar{\boldsymbol{b}}^+\mathbf{N}(\bar{\mathbf{A}}_1\mathbf{K}_1\bar{\mathbf{B}}_1 + \bar{\mathbf{A}}_2\mathbf{K}_2\bar{\mathbf{B}}_2)\mathbf{M}\bar{\boldsymbol{a}}\,\mathrm{d}\omega'\,\mathrm{d}\tau. \tag{23a}$$

Eqs. (3) and (4) and eqs. (10)–(23) constitute the final general results for the thermally averaged absorption lineshape and scattering cross section for the model outlined at the beginning of this section. When rotational motion is treated classically (when the experimental situation is such that no rotational structure is probed) the results (3) and (23) should be averaged over all molecular orientations. The model calculations presented in the next section are performed with the more simplified expressions (8) and (23a).

The thermal interaction of the molecule with its surroundings as well as nonthermal damping processes enter through the elements of $\bar{R}$ in the matrices $\mathbf{M}$, $\mathbf{N}$, $\mathbf{K}_1$ and $\mathbf{K}_2$. Contributions to $\bar{R}$ in eq. (7) arise from broadenings and shifts associated with different relaxation processes. Explicit forms are derived in appendices B and C of ref. [4]. There are three kinds of contributions: (a) Pure damping (irreversible decay of levels in manifold A) characterized by a damping matrix γ and level shift matrix $\mathbf{d}$. (b) Dephasing with rates denoted by elements of a matrix κ and associated shift matrix η. (c) Cross relaxation matrix Γ and its related shift $\mathbf{D}$. The rates appearing in Γ express the thermal transition rates between levels in the A manifold. Explicit expressions for these rates are provided in the appendix. Two points are worth noting: (a) The elements of the matrices γ, $\mathbf{d}$, κ, η, Γ and $\mathbf{D}$ are in principle frequency dependent. In the impact approximation one usually neglects this dependence but suitable frequency dependent models may be introduced [13] in order to study the implication of breakdown of the impact approximation. Also, at low T frequency dependence may become crucial, in view of relations (A.8)–(A.10). (b) Interference effects in the scattering cross section are always present when the manifold A contains more than one level. Interference effects in the lineshape originate from the nondiagonality of the matrices γ and $\mathbf{d}$.

For the simple case when the manifold A contains two levels r and s with $E_r > E_s$ (fig. 1), the absorption and scattering cross sections are obtained by applying eqs. (8) and (23a) with the radiative coupling matrices given by eqs. (14)–(21) (with $n = 2$, $a_1 \to r$, $a_2 \to s$) and with the thermally modified energy denominators M, N, K_1 and K_2 given by

$$\mathbf{M} = \begin{pmatrix} -\mathbf{m}^* & 0 \\ 0 & \mathbf{m} \end{pmatrix}, \tag{2}$$

$$\mathbf{m} = \begin{pmatrix} \tilde{E}_{rg}(E_0) - E_0 + \mathrm{i}\Gamma_r(E_0) & d_{rs} + \mathrm{i}\gamma_{rs} \\ d_{rs} + \mathrm{i}\gamma_{rs} & \tilde{E}_{sg}(E_0) - E_0 + \mathrm{i}\Gamma_s(E_0) \end{pmatrix}^{-1}. \tag{2}$$

$\mathbf{N}$ is obtained from $\mathbf{M}$ by replacing g and E_0 by g' and E_0';

$$\mathbf{K}_1 = \begin{pmatrix} 2\mathrm{i}(\Gamma_{rs} + \gamma_{rr}) & \mathrm{i}\gamma_{rs} + d_{rs} & \mathrm{i}\gamma_{rs} - d_{rs} & -2\mathrm{i}\Gamma_{rs}\exp(-\beta E_{rs}) \\ \mathrm{i}\gamma_{rs} + d_{rs} & \mathrm{i}(\gamma_{rr} + \gamma_{ss} + \kappa) - \tilde{E} & 0 & \mathrm{i}\gamma_{rs} - d_{rs} \\ \mathrm{i}\gamma_{rs} - d_{rs} & 0 & \mathrm{i}(\gamma_{rr} + \gamma_{ss} + \kappa) + \tilde{E} & \mathrm{i}\gamma_{rs} + d_{rs} \\ -2\mathrm{i}\Gamma_{rs} & \mathrm{i}\gamma_{rs} - d_{rs} & \mathrm{i}\gamma_{rs} + d_{rs} & 2\mathrm{i}[\Gamma_{rs}\exp(-\beta E_{rs}) + \gamma_{ss}] \end{pmatrix}, \tag{2}$$

and

$$\mathbf{K}_2 = \begin{pmatrix} (-E_{gg'} - E_0 + E' + \mathrm{i}\eta)^{-1} & 0 \\ 0 & (E_{gg'} + E_0 - E' + \mathrm{i}\eta)^{-1} \end{pmatrix}.$$

these equations

$$\gamma_{lm} = \sum \gamma^J_{lm}[\hbar^{-1}(E_g + E_0 - E_j)], \qquad d_{lm} = \sum d^J_{lm}[\hbar^{-1}(E_g + E_0 - E_j)]. \tag{28}$$

The energy dependence may be disregarded because $E_g + E_0 \gg E_j$ and the energy argument changes only slightly when E_0 covers the resonance region);

$$\Gamma_{rs} = \Gamma_{rs}(E_{rs}/\hbar) \qquad (E_{rs} = E_r - E_s > 0), \tag{29}$$

$$\tilde{E}_{rg}(E_0) = E_{rg} + d_{rr} + D_{rs}[\hbar^{-1}(E_g + E_0 - E_s)] + \eta_{rr}[\hbar^{-1}(E_g + E_0 - E_r)]. \tag{30}$$

$\tilde{E}_{sg}(E_0)$ is obtained by interchanging r and s in eq. (30);

$$\Gamma_r(E_0) = \Gamma_{rs}[\hbar^{-1}(E_g + E_0 - E_s)] + \gamma_{rr} + \kappa_{rr}[\hbar^{-1}(E_g + E_0 - E_r)], \tag{31a}$$

$$\Gamma_s(E_0) = \Gamma_{rs}[\hbar^{-1}(E_g + E_0 - E_r)] + \gamma_{ss} + \kappa_{ss}[\hbar^{-1}(E_g + E_0 - E_s)], \tag{31b}$$

$$\tilde{E} = E_{rs} + d_{rr} - d_{ss} + \eta. \tag{32}$$

Finally

$$\kappa = \kappa_{ss}(E_{rs}) + \exp(-\beta E_{rs})\kappa_{rr}(E_{rs}) - \kappa_{sr}(E_{rs}) - \kappa_{rs}(E_{rs}) \exp(-\beta E_{rs}), \tag{33a}$$

$$\eta = \eta_{ss}(E_{rs}) - \eta_{rr}(-E_{rs}) - \eta_{sr}(E_{rs}) + \eta_{rs}(-E_{rs}). \tag{33b}$$

The quantities appearing on the rhs of eqs. (28)–(33) are defined in the appendix. In obtaining these results, I have disregarded thermal relaxation of the g and g' levels.

To end this section, I consider the separation of the scattering cross section to its RRS and F contributions. When thermal relaxation processes involving the $|g\rangle$ and $|g'\rangle$ states are disregarded, the matrix $\mathbf{K}_2$ may be separated in the form

$$\mathbf{K}_2 = \begin{pmatrix} -1 & 0 \\ 0 & 1 \end{pmatrix} \mathrm{PP} \frac{1}{E_{gg'} + E_0 - E'} - i\pi \begin{pmatrix} 1 & 0 \\ 0 & 1 \end{pmatrix} \delta(E_{gg'} + E_0 - E'), \tag{34}$$

where PP denotes the principal part. It should be noticed that the structure of $\mathbf{K}_2$ in this approximation does not involve the intermediate manifold. Furthermore, a generalization of (34) may be obtained by replacing the δ function by a lorentzian with a width characterizing the relaxation of the $|g\rangle$ and $|g'\rangle$ levels (at least dephasing width should be anticipated). Inserting eq. (34) into eq. (23) leads to

$$\frac{\mathrm{d}^2(\sigma_{\lambda\nu})_{g\to g'}}{\mathrm{d}\omega' \,\mathrm{d}\tau} = \left(\frac{\mathrm{d}^2(\sigma_{\lambda\nu})_{g\to g'}}{\mathrm{d}\omega' \,\mathrm{d}\tau}\right)^{\mathrm{RR}} + \left(\frac{\mathrm{d}^2(\sigma_{\lambda\nu})_{g\to g'}}{\mathrm{d}\omega' \,\mathrm{d}\tau}\right)^{\mathrm{F}}, \tag{35}$$

where

$$\left(\frac{\mathrm{d}^2(\sigma_{\lambda\nu})_{g\to g'}}{\mathrm{d}\omega' \,\mathrm{d}\tau}\right)^{\mathrm{RR}} = -\frac{2}{c^4}\omega_0\omega'^3 \bar{b}^+_\lambda \mathbf{N}(\bar{\mathbf{A}}_2)_\nu(\bar{\mathbf{B}}_2)_\lambda \mathbf{M}a_\nu \delta(\omega_{gg'} + \omega_0 - \omega'), \tag{36}$$

is the Raman scattering cross section and where

$$\left(\frac{\mathrm{d}^2(\sigma_{\lambda\nu})_{g\to g'}}{\mathrm{d}\omega' \,\mathrm{d}\tau}\right)^{\mathrm{F}} = -\frac{2\hbar}{\pi c^4}\omega_0\omega'^3 \bar{b}^+_\lambda \mathbf{N}\left[(\mathbf{A}_1)_\lambda \mathbf{K}_1(\bar{\mathbf{B}}_1)_\nu + \mathrm{PP}\frac{1}{E_{gg'} + E_0 - E'}(\bar{\mathbf{A}}_2)_\nu \begin{pmatrix} -1 & 0 \\ 0 & 1 \end{pmatrix} (\bar{\mathbf{B}}_2)_\lambda\right] \mathbf{M}a_\nu \tag{37}$$

is the cross section for resonance fluorescence. Under the conditions which lead to eq. (23a) I get

$$\left(\frac{\mathrm{d}\sigma_{g\to g'}}{\mathrm{d}\omega'}\right)^{\mathrm{RR}} = -\frac{4\pi}{c^4}\omega_0\omega'^3 \bar{b}^+ \mathbf{N}\bar{\mathbf{A}}_2\bar{\mathbf{B}}_2\mathbf{M}\bar{a}\delta(\omega_{gg'} + \omega_0 - \omega'), \tag{38}$$

and

$$\left(\frac{d\sigma_{gg'}}{d\omega'}\right)^F = -\frac{4\hbar}{c^4}\omega_0\omega'^3\bar{b}^+\mathbf{N}\left[\bar{\mathbf{A}}_1\mathbf{K}_1\bar{\mathbf{B}}_1 + \mathrm{PP}\frac{1}{E_{gg'}+E_0-E'}\bar{\mathbf{A}}_2\begin{pmatrix}-1 & 0\\ 0 & 1\end{pmatrix}\bar{\mathbf{B}}_2\right]\mathbf{M}a, \tag{39}$$

where I have also assumed directional uniformity of the scattered radiation (as would be the case for the simplified model if the molecules are freely rotating and no rotational structure is probed) and substituted a factor of 4π for angular integration.

It should be noticed that the fluorescence cross section [eqs. (37) and (39)] includes both resonance fluorescence (direct) lines resulting from levels approximately in resonance with the exciting beam and ordinary fluorescence (transfer) lines originating from levels which are populated in course of the thermal relaxation process. Physically both contributions result from thermal interactions and are treated on equal footing.

Eqs. (8), (18)–(26) and (38)–(39) are the basis for the model calculations described in the next section.

3. Model calculations and discussion

The numerical calculations described here provide apart from the energy dependent absorption, RRS and RF cross sections also the quantities

$$y(\omega_0) = \frac{1}{\sigma_g}\int d\omega'\left[\left(\frac{d\sigma_{g\to g'}}{d\omega'}\right)^{RR} + \left(\frac{d\sigma_{g\to g'}}{d\omega'}\right)^{F}\right], \tag{40}$$

which is the total (energy resolved) quantum yield for emission into the molecular state g', and

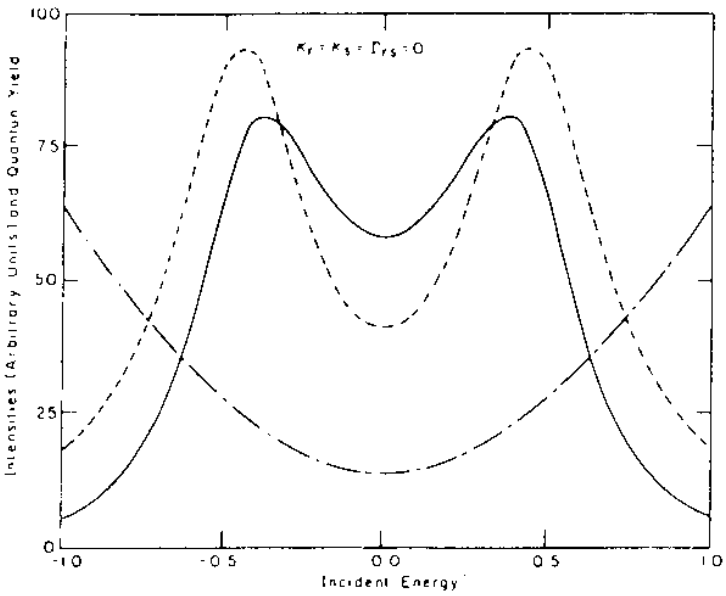

Fig. 3. Absorption lineshape (———) × 3, scattering cross section (– –) × (5 × 10^2) and total quantum yield (— · —) × 10^4 as functions of incident energy for an isolated molecule (no thermal relaxation) with intramolecular damping $\gamma_{rr} = \gamma_{ss} = 0.25$. $\mu_{gr} = \mu_{gs} = \mu_{g'r} = \mu_{g's}$ chosen such that the radiative widths of levels r and s are 0.00125. The energy scale is set relative to $E_r - E_s = E_{rs}$, which is taken to be 1. The origin is chosen so that $\frac{1}{2}(E_r + E_s) = 0$. Energy shifts are disregarded (or absorbed into E_{rs}). $\gamma_{rs} = -0.23$, the negative sign implies constructive interference in the absorption lineshape between the two absorption peaks.

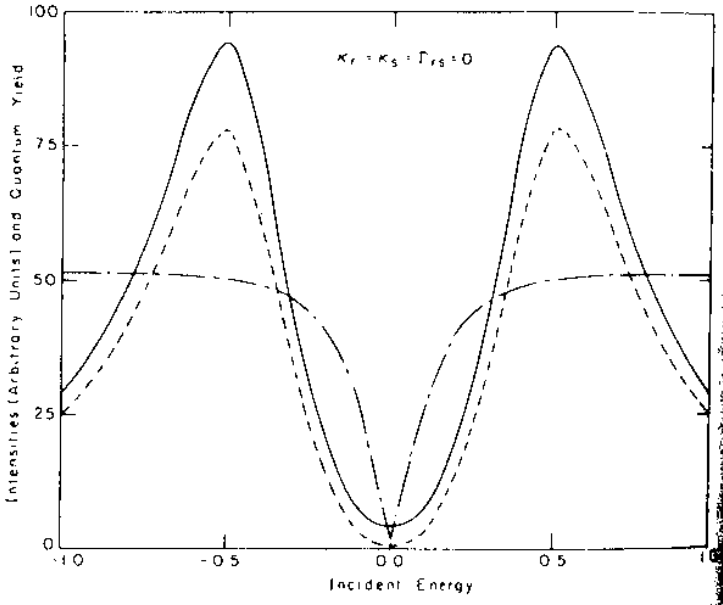

Fig. 4. Isolated molecule. Parameters and scale factors are identical to those in fig. 3 apart from the choice of $\gamma_{rs} = 0.23$. The positive sign of γ_{rs} implies destructive interference between two absorption maxima.

$$R(\omega_0) = \left[\int d\omega' \left(\frac{d\sigma_{g\to g'}}{d\omega'}\right)^{RR}\right]\left[\int d\omega' \left(\frac{d\sigma_{g\to g'}}{d\omega'}\right)^{F}\right]^{-1}, \tag{41}$$

the ratio between the integrated resonance Raman and resonance fluorescence cross sections.

I have studied the effect of thermal relaxation on simple interference structures. The first (figs. 3 and 4) is the interference pattern resulting when the intermediate manifold A consists of two closely lying levels. Fig. 5 shows the effects of thermal relaxation processes on the various cross sections and cross section ratios as functions of the incident photon energy, while figs. 6 and 7 display the effect on the differential cross section represented as functions of the scattered photon energy. Parameters are as given under the figures where the energy scale is set by choosing $E_r - E_s = 1.0$. In figs. 6 and 7 the scattered energy is shifted relative to the incident one by the amount $E_{g'} - E_g$ so that both can be represented on the same figure.

A second interference pattern (fig. 8) is obtained by choosing the radiative couplings and the non-radiative widths of the levels $|s\rangle$ and $|r\rangle$ such as to give the effect of an optically active intermediate level interacting with an optically active continuum. This results in a typical Fano interference pattern [14] which is affected by thermal relaxation processes as shown in figs. 8 and 9. In fig. 9 the arrows mark a position shifted by $E_{gg'}$ from the incident photon energy, where a Raman δ-shape component is located. For the parameters used the scattered spectrum is independent of the excitation energy. The two arrows correspond to two different calculations.

Figs. 3–9 are obtained in the high temperature limit ($k_bT = 100$). Figs. 10–12 display the temperature effect on the scattering process. Here the parameters are chosen so as to minimize interference between the two

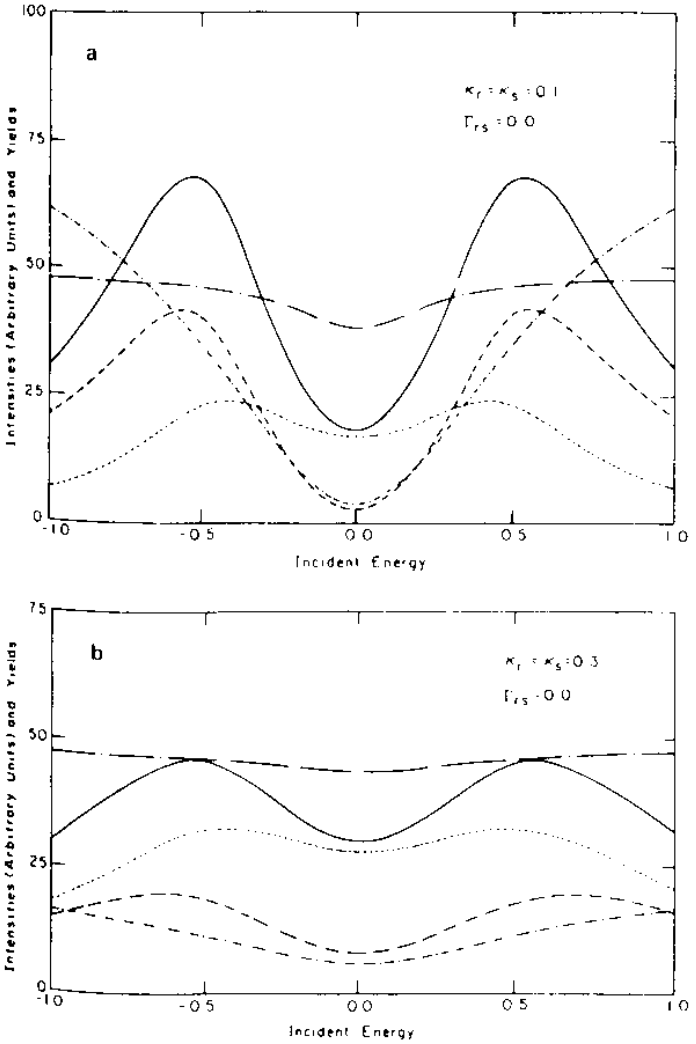

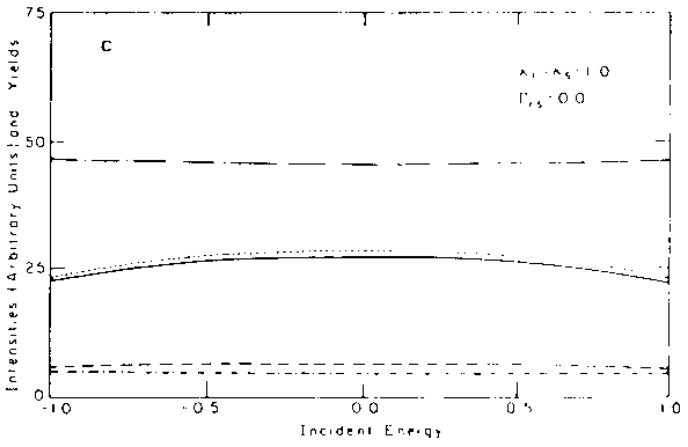

Fig. 5. Absorption lineshape (———) × 3, Raman scattering (– – –) × (5×10^2), integrated fluorescence (——) × 10^3, R (– · –) × 10 and total quantum yield (— · —) × 10 as functions of incident photon energy. γ_{rr}, γ_{ss}, γ_{rs}, E_{rs} and the μ's as in fig. 4. In addition κ_{rr} κ_{ss} = 0.1 (a), 0.3 (b) and 1.0 (c), $k_BT = 100$ and $\Gamma_{rs} = 0$. Taking $\kappa_{rr} = \kappa_{ss} = 0$ and $\Gamma_{rs} = 0.1, 0.3, 1.0$ essentially reproduce the behavior in (a), (b) and (c).

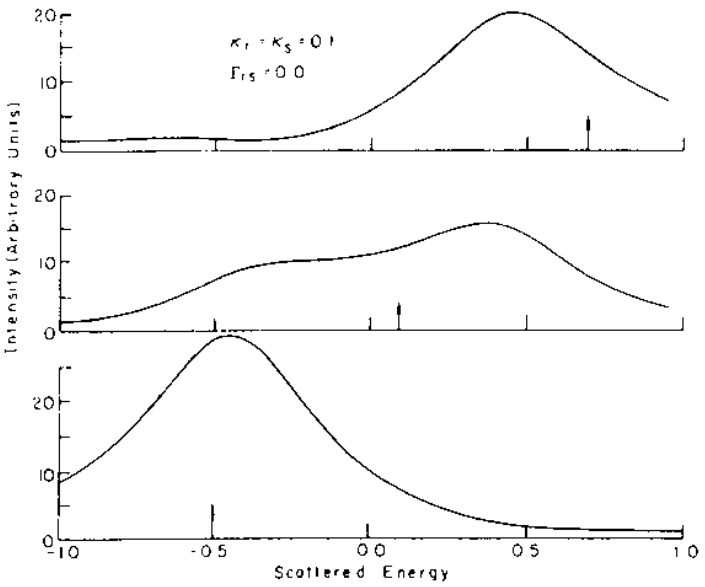

Fig. 6. Scattered intensity as a function of scattered energy. Parameters are chosen as in fig. 4 with $\Gamma_{rs} = 0$, $\kappa_{rr} = \kappa_{ss} = 0.1$, $k_B T = 100$. The Raman component of the scattered radiation is a δ function peak (not shown) at the position of the arrow (its lack of width results from the neglect of thermal relaxation of the g, g' levels). The incident energy is given by the position of the arrow shifted by $E_{gg'}$. The ratio between the integrated Raman and the integrated fluorescence intensities for any given incident energy is the R curve of fig. 5.

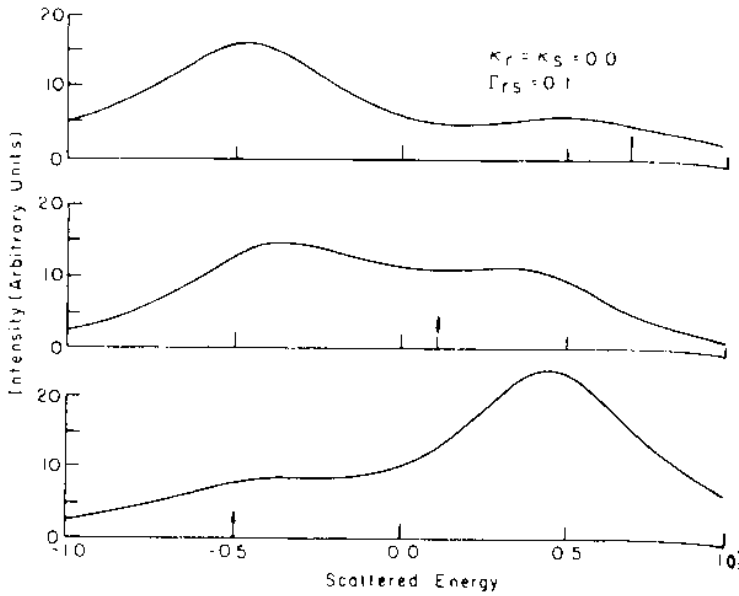

Fig. 7. Scattered intensity as a function of scattered energy. Parameters as in fig. 6 only now $\kappa_{rr} = \kappa_{ss} = 0$ and $\Gamma_{rs} = 0.1$.

levels. Because of limitations on the validity of the separation approximation used here, the calculation is meaningful only provided $k_B T > \Gamma_r, \Gamma_s$, where Γ_r and Γ_s are given by eq. (31). Thermal effects, however, become pronounced once $k_B T$ becomes of the order of E_{rs} ($= 1$ here).

The following conclusions can be reached from this numerical study.

(1) Interference effects lead to a nontrivial incident energy dependence of the total quantum yield $Y(\omega)$. As parameters where chosen symmetrically between the individual resonances $|r\rangle$ and $|s\rangle$, the energy dependence observed in figs. 3–5 results only from interference. $Y(\omega)$ is seen to attain a minimum at the points of maximum interference in figs. 3–5 and a maximum at the center of the Fano interference feature (fig. 8). Interference effects on the energy dependence of the quantum yield function have been previously studied by us [16] and have since been experimentally observed [20–26].

(2) Thermal relaxation processes, expressed in figs. 5 and 8 by increasing dephasing width κ_{rr} and κ_{rs} erase the interference character of the lineshapes. This is seen in several ways: (a) In the cases studied in figs. 4 and 5, the quantum yield function becomes almost energy independent much before there is a marked change in the absorption and RRS spectrum. (b) In fig. 5, while the RRS spectrum follows qualitatively the absorption lineshape, the F component shows a qualitatively different behavior, lacking any interference character. This may have been anticipated as the F component arises from the non-coherent thermal interaction. (c) A similar effect is seen in the Fano feature (fig. 8): while the absorption lineshape is markedly asymmetric and the Raman component shows some degree of asymmetry, the F component is completely symmetrical about the center of the feature.

(3) When thermal broadening becomes large (fig. 5c) the absorption, Raman and fluorescence components become broad, having a maximum at the center of the spectral feature.

(4) The ratio R between the integrated RRS and F components also displays the effects of interference. In the impact approximation, essentially used in this work, R is expected to be independent of the incident photon

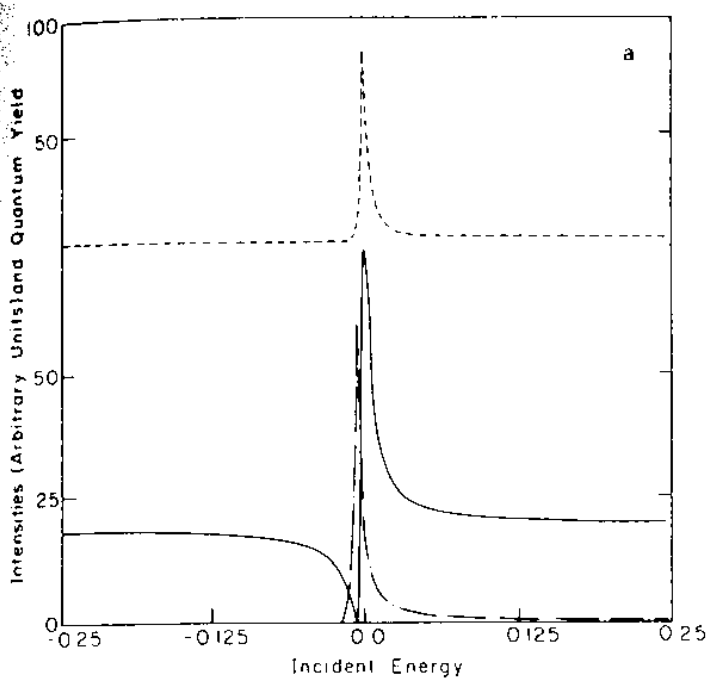

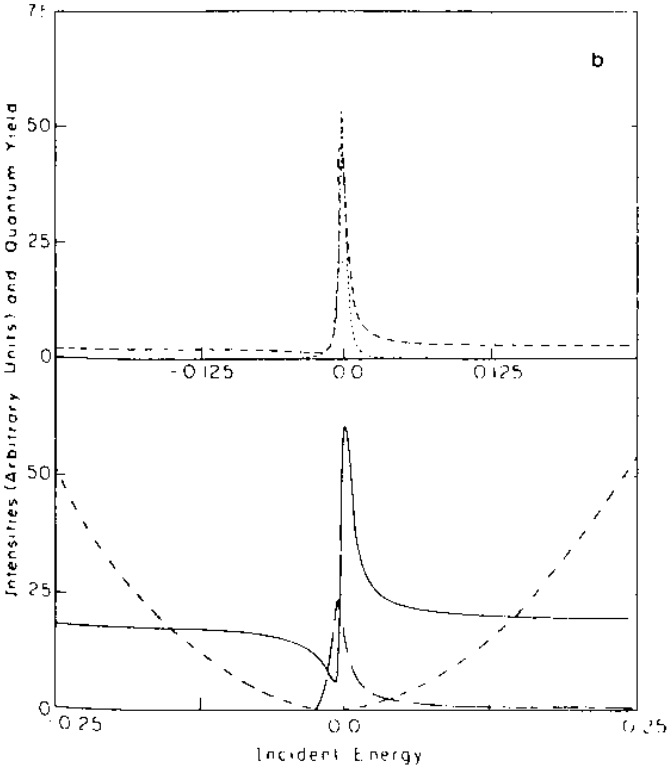

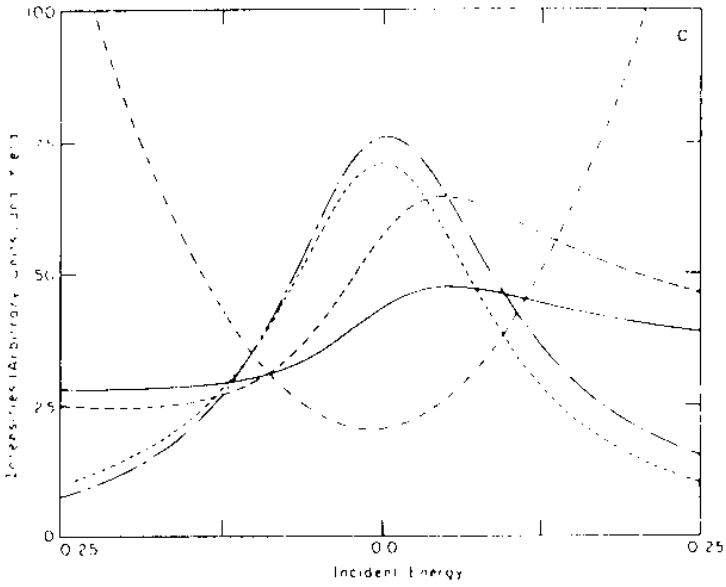

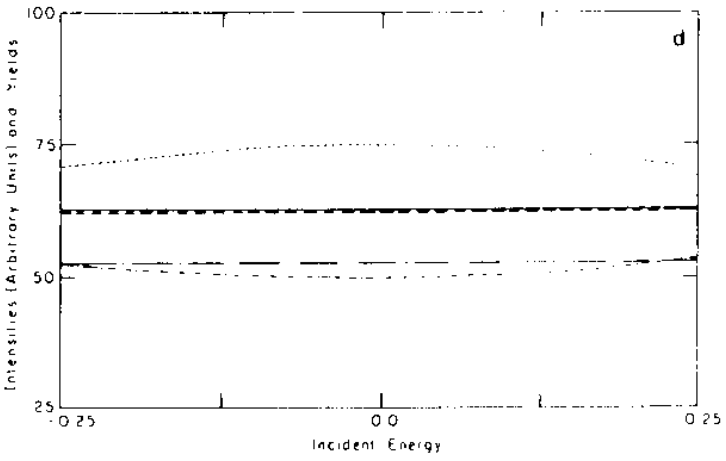

Fig. 8. Absorption lineshape (———), Raman scattering cross section (— · · · —), integrated fluorescence (– – –), R (– · –) and total quantum yield (— · —) as functions of incident photon energy. Parameters are chosen to produce a typical Fano lineshape: $\gamma_{ss} = 50.0049$, $\gamma_{rr} = 50.0051$, $\gamma_{sr} = 50.0050$; radiative width (for emission to g) of $|s\rangle$ is 0.0049, of $|r\rangle$ is 0.0051, $k_B T = 100$. (a) Isolated molecule, $\kappa_{rr} = \kappa_{ss} = 0$. Scale factors: Absorption $\times 30$, RRS $\times (4 \times 10^4)$. The quantum yield plot is for the function $(\log_{10} QY + 4) \times 20$. (b) $\kappa_{rr} = \kappa_{ss} = 0.001$. Scale factors: Absorption, RRS and quantum yield – as in (a); F $\times 10^5$, R $\times (5 \times 10^{-2})$. (c) $\kappa_{rr} = \kappa_{ss} = 0.1$. Scale factors: Absorption $\times 10^2$, RRS $\times 10^6$, F $\times (2 \times 10^6)$, $Y \times (5 \times 10^5)$, $R \times 10$. (d) $\kappa_{rr} = \kappa_{ss} = 1.0$. Scale factors: Absorption $\times 10^2$, RRS $\times 10^6$, F $\times (2 \times 10^7)$, $Y \times (5 \times 10^5)$, $R \times 3$.

energy while in reality R grows towards the band tails. The energy dependence of R shown in figs. 5 and 8, arises from interference and disappears quickly with the increase in the thermal relaxation rates.

(5) In the two-intermediate level interference case (figs. 4 and 5) the effect of cross-relaxation process ($\Gamma_{rs} > 0$) on the incident energy dependence of the different cross sections and cross section ratios is qualitatively and quantitatively similar to that of level dephasing ($\kappa_{rr}, \kappa_{ss} > 0$). Usually dephasing rates are much larger than cross relaxation rates.

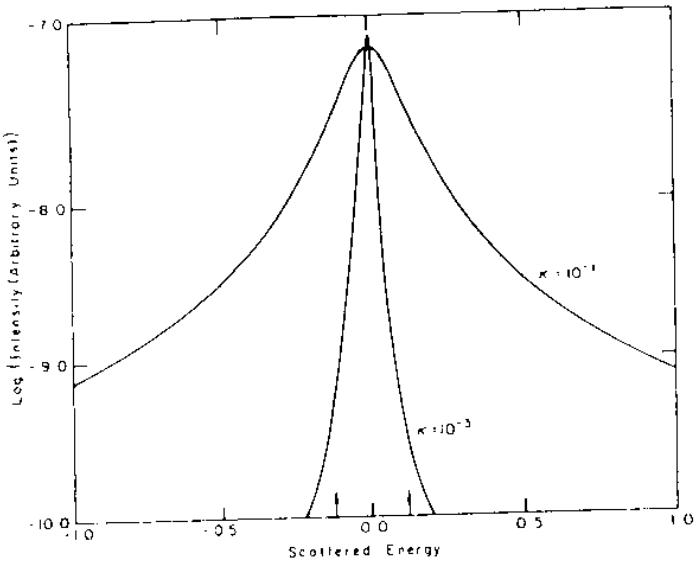

Fig. 9. Scattered intensity as a function of scattered energy. The parameters are like in figs. (8b) and (8c). Different incident photon energies (shifted by $E_{g'}-E_g$ from the positions of the arrows) make no effect on the fluorescence spectrum shown. In addition there is a δ function Raman component (not shown) located at the position of the arrow (the two arrows indicate two different calculations with two different incident energies).

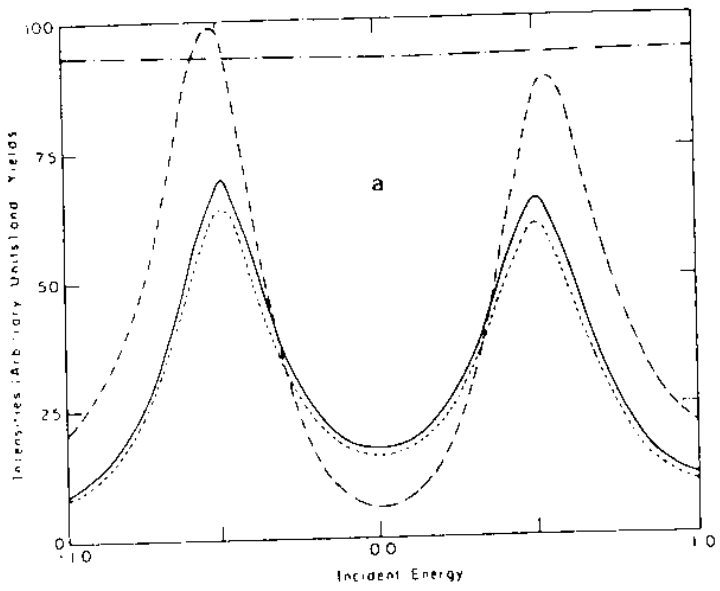

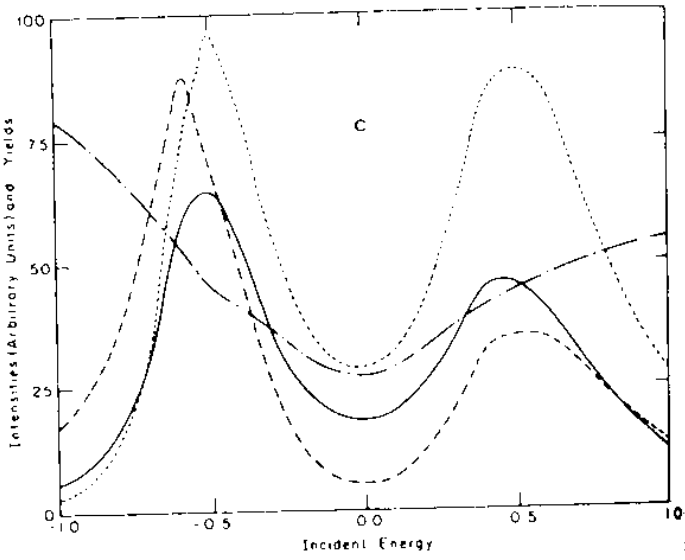

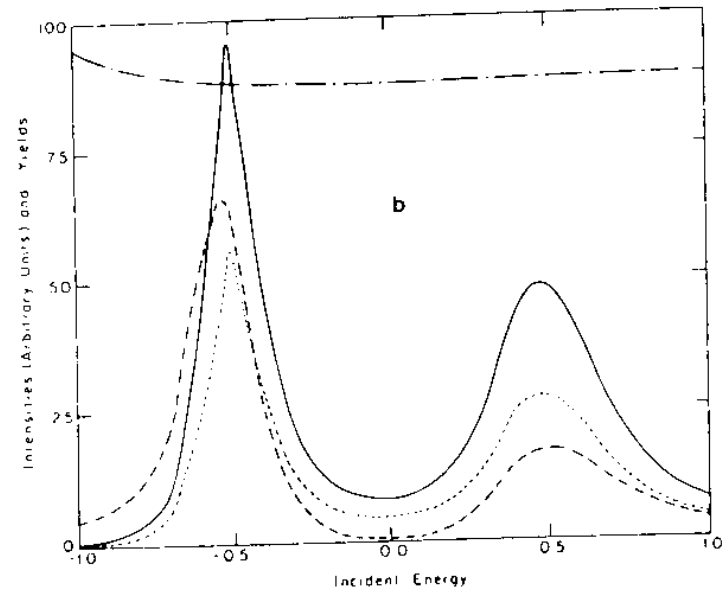

Fig. 10. Absorption lineshape (———), Raman scatter (— — —), integrated fluorescence (– – –) and total qua yield (–·–) as function of incident photon energy. μ_{rg}, $\mu_{rg'}$ and μ_{sg}, $\mu_{sg'}$ correspond to radiative widths (emission to the g and to the g' channels) of 10^{-4}. $E_{rs} = 1.0$, $\Gamma_{rs} = \kappa_{rr} = \kappa_{ss} = 0.1$, $\gamma_{rs} = 0$. (a) $k_BT = 10$, $\gamma_{ss} = \gamma_{rr} = 10^{-3}$. Scale factors: Absorption × 20, RRS × (5×10^4), F × (2×10^2), $Y \times 10^3$. (b) $k_BT =$ $\gamma_{ss} = \gamma_{rr} = 10^{-3}$. Scale factors: Absorption × 15, RRS × 10^4, F × 10^2, $Y \times 10^3$. (c) $k_BT = 0.3$, $\gamma_{ss} = \gamma$ = 0.1. Scale factors: Absorption × 20, RRS × (4 × F × (8×10^4), $Y \times (5 \times 10^4)$.

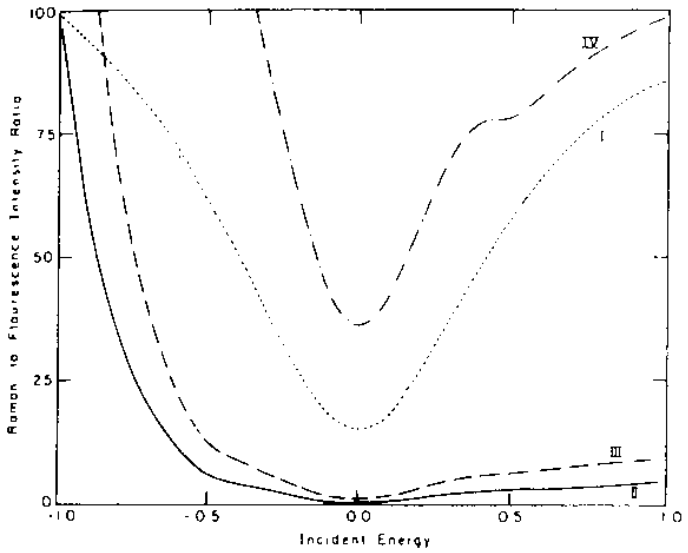

Fig. 11. R, the ratio between the integrated Raman and the integrated fluorescence cross sections, as a function of incident photon energy. Parameters are as in fig. 10 with (I) $k_BT = 10$, $\gamma_{rr} = \gamma_{ss} = 10^{-3}$ $(R \times 10^4)$; (II) $k_BT = 0.3$, $\gamma_{rr} = \gamma_{ss} = 10^{-3}$ $(R \times 5 \times 10^2)$; (III) $k_BT = 0.3$, $\gamma_{rr} = \gamma_{ss} = 10^{-2}$ $(R \times 10^2)$; (IV) $k_BT = 0.3$, $\gamma_{rr} = \gamma_{ss} = 10^{-1}$ $(R \times 10^2)$.

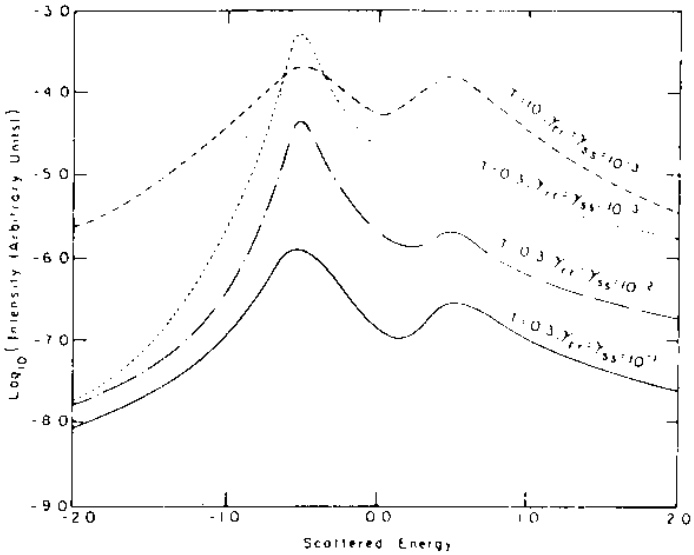

Fig. 12. Scattered intensity as a function of scattered energy. Parameters are like figs. (10) and (11). For these parameters the spectral distribution does not depend on the incident energy (apart from an increase of the overall intensity when the absorption cross section increases). Shifted by $E_{gg'}$ from the incident energy there is a δ shape Raman component which is not shown in the figure.

(6) The scattered intensity monitored as a function of scattered energy (figs. 6–8) reveals a δ-shape component shifted by $E_{gg'}$ from the incident photon energy (at the positions marked by arrows in the figures) and an energy dispersed fluorescence component. The zero width of the Raman component results from neglecting relaxation of the $|g\rangle$ and $|g'\rangle$ levels. The fluorescence component consists of direct lines (originating from the level most closely in resonance with the incident radiation) and transfer lines. It is seen from figs. 6 and 7 that κ_{rr} and κ_{ss} enhance the intensity of direct lines while Γ_{rs} enhances the intensity of transfer lines.

(7) The scattered intensity monitored as a function of scattered energy, in the case of a Fano interference feature (fig. 9) is symmetric around the center of the feature, in contrast to the incident energy dependence of the absorption and Raman lineshapes displayed in fig. 8, but in agreement with the incident energy dependence of the F component.

Turning now to the temperature dependence study (figs. 9–12) we observe the following points:

(8) Figs. 10a and 10b indicate that as the temperature becomes lower the lineshapes become asymmetric even when all radiative couplings and relaxation parameters are chosen equal for the $|r\rangle$ and $|s\rangle$ levels. The lineshapes associated with the lower $|s\rangle$ level are narrower than those originated from the $|r\rangle$ level. Similar effect is shown by the fluorescence spectrum (fig. 12). This is caused by the cross relaxation, Γ_{rs}, process which for lower temperatures becomes less reversible. At the zero T limit it will contribute a damping (as opposed to thermal) width to the level $|r\rangle$ and no width at all to $|s\rangle$. When other damping channels become more effective (γ_{rr}, γ_{ss} increase, fig. 10c) this effect becomes less pronounced.

(9) The energy independence of the quantum yield function in the cases represented by figs. 10a and 10b indicates that interference effects do not play an appreciable role there. When the damping widths γ_{rr} and γ_{ss} become larger (fig. 10c), the resonances overlap, and interference in the scattering cross sections makes Y energy dependent. Note that overlap of the resonances resulting from thermal broadening (κ_{rr}, κ_{ss} and Γ_{rs} in figs. 10a and 10b are of the same magnitude as γ_{rr}, γ_{ss} in fig. 10c) does not lead to interference.

(10) The ratio R between the integrated RRS and F components shown in fig. 11 as a function of incident energy shows three interesting effects: (a) R has a minimum at the center of the spectral feature. This is essentially an interference effect as discussed above. (b) The rise in R for lower energies, more pronounced at

lower temperatures, results from the energy dependence of the thermal relaxation rates as expressed by eq. (A.8) and (A.10). At low temperature the widths associated with the thermal processes disappear and the scattering process becomes more coherent. (c) R increases when the damping processes (expressed by γ_{rr} and γ_{ss}) become more efficient. This effect was discussed in detail in ref. [4], and is the basis for the use of quenchers in order to eliminate fluorescence components from Raman spectra. It is interesting to note that adding a foreign gas as a quencher to the irradiated sample may have two opposing effects. On one hand, it may enhance the thermal relaxation processes (vibrational and rotational relaxation and collision broadening) and increase the rates Γ_{rs}, κ_{rr}, κ_{ss}; on the other hand, it may irreversibly quench the excited electronic state thus enhancing γ_{rr} and γ_{ss}. The first effect will lead to a decrease, while the second to an increase in R. The net effect depends on the relative efficiency of the added gas as a thermal relaxation agent and as an electronic quencher.

At present, theoretical analysis of RRS experiments is mostly based, even for thermally interacting systems on the conventional expression (1) which is suitable only for isolated molecules. A proper treatment of thermal effects has been provided before only for a single intermediate level [5] (or a quasi-degenerate set of intermediate levels [6]), and the results indicate that eq. (1) indeed cannot be used. Theoretical fits to experimental results from which parameters like γ are extracted are therefore doubtful.

Recently, Penner and Siebrand [31] and Mortensen [32], have attempted to take solvent broadening effects in the analysis of models constructed for RRS from MnO_4^- and from β carotene in solutions. The approach of these authors is based on taking a convolution integral of eq. (1) with a lorentzian function with a width associated with the medium broadening. In view of the results presented here and in ref. [4], this is clearly not sufficient as a general method. It may be shown however that this approach leads to the correct result for the excitation spectrum (but not for the spectrum of the scattered radiation) in the absence of interference effects and provided that level dephasing is the only thermal effect of importance (population relaxation disregarded). The later condition is realized, for example, if irreversible damping is much faster than population relaxation between emitting levels but slower than or of the same order as the rate of dephasing. It is important to notice that even in that simplified approach, the medium broadening effects on the excitation spectrum, and particularly on the depolarization spectrum, are shown to be significant.

Eqs. (35)–(37) provide the formal basis for the separation of the light scattering cross section into its coherent RRS part and non-coherent F part. This is a generalization of Huber's result [5] for the single resonance case. Huber's formula has been used for the analysis of experimental results in the multilevel I_2 resonance light scattering experiment [33]. Such an application will fail when interference effects and/or transfer lines play an appreciable role in the observed spectrum, and indeed it cannot account for a few features in the I_2 spectrum. Eqs. (35)–(37) provide an appropriate tool for analysis of light scattering experiments in thermally relaxing multilevel systems. When the levels in the intermediate manifold contribute independently of each other (interference and population transfer negligible) our results reduce to a sum of contributions of the Huber type [4].

The relative intensities of the RRS, RF and regular fluorescence contributions to the scattered spectrum yield information on the thermal relaxation rates. Example for the way in which such information can be obtained is provided in ref. [4]. In practice one can resolve these separate contributions only in very simple systems. Quantitative measurements in a one intermediate level system were done only very recently [3]. Atoms which are studied in level crossing experiments suggest themselves as two intermediate level systems (e.g. the 2^3P_1 and 2^3P_2 states of helium) for which the results of section 2 will be directly applicable. Such cases are particularly attractive because the intermediate level separation, controlled by an external magnetic field, is an additional experimental variable.

In more complicated systems, eqs. (35)–(37) rather than eq. (1) should be used for fitting the experimental spectra. Only the total scattering cross section (and, using the absorption spectrum – the total quantum yield) will be a measurable observable. An additional observable is provided by the energy resolved depolarization ratio which can also be analysed using eqs. (35)–(37). It should be mentioned that a complete analysis of these observables should involve also a thermal averaging over the distribution of initial molecular states (in such

high temperatures where the population of excited states in the ground electronic manifold become appreciable). At a low enough pressure one may also need to take account of the Doppler broadening by convoluting the results obtained here with a suitable gaussian function.

4. Conclusion

In this paper I have provided a general working expression for the cross section of resonance light scattering in thermally relaxing systems. This cross section consists of RRS and fluorescence (resonance and regular) contributions and should replace the conventional expression (eq. (1)) for RRS which is suitable only for isolated systems. Numerical calculations indicate that thermal relaxation processes have an appreciable influence of the excitation and the scattering spectra. Analysis of these spectra will yield information on these relaxation processes.

Acknowledgement

I am grateful to Professors A. Ben Reuven and J. Jortner for many helpful discussions and to I. Ran for performing the numerical computations reported in this paper.

Appendix: Relaxation rates and associated level shifts

The light scattering molecule is characterized by the levels $|g\rangle$, $|g'\rangle$ and the intermediate manifold $A \equiv \{|a\rangle\}$. Relaxation phenomena may be described by introducing two distinct baths. First a thermal bath of temperature T with a system–bath interaction operator which may be expanded in the form

$$U_T = U_1 + U_2, \tag{A.1}$$

$$U_1 = \sum_{\substack{a \\ a \neq a'}} \sum_{a'} F_{aa'} |a\rangle \langle a'|, \tag{A.2}$$

$$U_2 = \sum_a K_a |a\rangle \langle a| + K_g |g\rangle \langle g| + K_{g'} |g'\rangle \langle g'|. \tag{A.3}$$

$F_{aa'}$ and K_i are operators in the bath coordinates. I assume that bath correlation functions of the kind $\langle FK \rangle$ vanish. Thus the diagonal and the non-diagonal parts of U_T may be thought of as formally originated from two different thermal baths.

Secondly, irreversible damping of levels in A may be associated with a zero temperature bath seated on some lower molecular level $|j\rangle$. The molecular bath interaction is of the form

$$U_J = \sum_a (J_{ja} |j\rangle \langle a| + J_{aj} |a\rangle \langle j|). \tag{A.4}$$

There may be several damping channels each leading to a different final level j and each corresponding to a different U_J. J_{ja} are operators in the coordinates of the zero temperature bath. It should be kept in mind that the "zero temperature bath" does not usually correspond to a physical thermal bath. Two common examples are intramolecular radiationless transitions where j corresponds to a lower electronic level and the bath is the manifold of vibrational states associated with it; and the related problem of medium induced electronic relaxation where the bath is the surrounding medium and as such identical to that inducing U_T, however, because electronic energy gaps are usually much larger than $k_B T$, the medium will have the effect of a zero temperature bath.

The relevant relaxation rates and level shifts are obtained as Fourier–Laplace transforms of time correlation functions of bath operators†

$$\int_0^\infty dt \exp(i\omega t) \langle J_{aj}(t) J_{ja'}(0) \rangle = \gamma^J_{aa'}(\omega) + i d_{aa'}(\omega), \tag{A.5}$$

$$\int_0^\infty dt \exp(i\omega t) \langle F_{aa'}(t) F_{a'a}(0) \rangle = \Gamma_{aa'}(\omega) + i D_{aa'}(\omega), \tag{A.6}$$

$$\int_0^\infty dt \exp(i\omega t) \langle K_l(t) K_m(0) \rangle = \kappa_{lm}(\omega) + i\eta_{lm}(\omega). \tag{A.7}$$

The relaxation rates satisfy the detailed balance relations

$$\Gamma_{aa'}(-\omega) = \exp(-\beta\omega)\Gamma_{aa'}(\omega), \tag{A.8}$$

$$\gamma^J_{aa'}(-\omega) = 0, \tag{A.9}$$

$$\kappa_{lm}(-\omega) = \exp(-\beta\omega)\kappa_{lm}(\omega). \tag{A.10}$$

Temperature dependence is obtained in this formalism through these relations.

† Note the difference in notation from ref. [4]: (a) $\Gamma_{aa'}$ and $D_{aa'}$ are identical to $\Gamma'_{aa'}$ and $D'_{aa'}$ there; (b) $\gamma^J_{aa'}$ and $d^J_{aa'}$ are identical for $a = a'$ to Γ'_{aj} and D'_{aj} there, and for $a \neq a'$ to γ'_j, d'_j there. (c) κ_{lm} here is identical to κ'_{lm} there.

References

[1] P.P. Shorygin, Soviet Phys. USP 16 (1973) 99;
W. Kiefer, Appl. Spectry. 28 (1974) 115;
J. Behringer, in: Molecular spectroscopy, Vols. 2 and 3, eds. R.F. Barrow, D.A. Long and J.J. Miller (The Chemical Society, London 1974, 1975).
[2] D.L. Rousseau and P.F. Williams, J. Chem. Phys. 64 (1976) 3519.
[3] J.L. Carlsten, A. Szöke and N.G. Raymer, Phys. Rev. A15 (1977) 1029.
[4] S. Mukamel and A. Nitzan, J. Chem. Phys. 66 (1977) 2462.
[5] D.L. Huber, Phys. Rev. 158 (1967) 843; 170 (1968) 418; 178 (1969) 93; 178 (1969) 392.
[6] A. Omont, E.W. Smith and J. Cooper, Astrophys. J. 175 (1972) 185; 182 (1973) 283.
[7] V. Hizhnyakov and I. Tehver, Phys. Stat. Sol. 21 (1977) 755.
[8] K. Rebane and P. Saari, J. Luminescence 16 (1978) 223.
[9] V. Hizniakov, ISSP Technical Report A860 (Tokyo, 1977).
[10] I. Rebane, Proceedings of the Estonian Academy of Sciences (USSR) 27 (1978) 192.
[11] T. Takagahara, E. Hanamura and R. Kubo, J. Phys. Soc. Japan, 43 (1977) 802, 1522; 44 (1978) 728, 742.
[12] G. Nienhius, Physica 81C (1976); 85C (1977) 151; 93C (1978) 393.
[13] G. Nienhius and F. Schuller, Physica 92C (1977) 397, 409; 94C (1978) 394.
[14] Y.R. Shen, Phys. Rev. B9 (1974) 622.
[15] R.M. Hochstrasser and F.A. Novak, Chem. Phys. Letters 41 (1976) 407; 48 (1977) 1; 53 (1978) 3.
[16] A. Nitzan and J. Jortner, J. Chem. Phys. 57 (1972) 2870.
[17] O.S. Mortensen, J. Mol. Spectry. 171 (1971) 39, 48.
[18] C. von Grundherr and M. Stockburger, Chem. Phys. Letters 22 (1973) 254.
[19] A. Ranade and M. Stockburger, Chem. Phys. Letters 22 (1973) 257.
[20] J. Friedman and R.M. Hochstrasser, Chem. Phys. Letters 32 (1975) 414.
[21] A.R. Gregory, W.H. Henneker, W. Siebrand and M.Z. Zgierski, J. Chem. Phys. 63 (1975) 5475.
[22] R. Liang, O. Schnepp and A. Warshel, Chem. Phys. Letters 44 (1976) 394.

[23] S. Hassing and O. Mortensen, Chem. Phys. Letters 47 (1977) 115.
[24] M.Z. Zgierski, J. Raman Spectry. 6 (1977) 53.
[25] J.M. Friedman, D.L. Rousseau and V.E. Bondybey, Phys. Rev. Letters 37 (1976) 1610.
[26] P. Baierl, W. Kiefer, P.F. Williams and D.L. Rousseau, Chem. Phys. Letters 50 (1977) 57.
[27] E. Courtens and A. Szöke, Phys. Rev. A15 (1977) 1588, and reference therein.
[28] M. Jacon and D. van Labeke, Mol. Phys. 29 (1975) 1241.
[29] S.D. Druger, J. Chem. Phys. 67 (1977) 3238, 3249.
[30] B. Carmeli and A. Nitzan, to be published.
[31] A.P. Penner and W. Siebrand, Chem. Phys. Letters 39 (1976) 11.
[32] O.S. Mortensen, Chem. Phys. Letters 43 (1976) 576.
[33] D.L. Rousseau, G.D. Patterson and P.F. Williams, Phys. Rev. Letters 34 (1975) 1306.